Integration of machine learning prediction and optimization for determination of the coefficient of friction of textured UHMWPE surfaces

Feng, Huihui; Liu, Jing Sheng; van Ostayen, Ron; Ji, Cuicui; Xu, Haoran

DOI
10.1177/13506501241272816

Publication date
2025

Document Version
Final published version

Published in
Proceedings of the Institution of Mechanical Engineers, Part J: Journal of Engineering Tribology

Original Article

Institution of MECHANICAL ENGINEERS
Journal of ENGINEERING TRIBOLOGY

Proc IMechE Part J: J Engineering Tribology
2025, Vol. 239(2) 173–188

DOI: 10.1177/13506501241272816
journals.sagepub.com/home/pij
Sage

Integration of machine learning prediction and optimization for determination of the coefficient of friction of textured UHMWPE surfaces

Huihui Feng[1,2], Jing Liu[1], Ron van Ostayen[2], Cuicui Ji[1] and Haoran Xu[1]

Abstract

The frictional performance of water-lubricated UHMWPE is influenced by the combination of structural parameters and operating conditions. To improve the efficiency of optimal design of surface texture aimed at improving frictional performance, a novel integration of the Orthogonal Array method (OAM), machine learning (ML) prediction, and Particle Swarm Optimization (PSO) is proposed for predicting and optimizing the coefficient of friction (COF) of copper ball-textured UHMWPE surfaces using a small dataset. In order to reduce manufacturing and testing cost, decrease required training samples for ML algorithm, OAM which could efficiently acquire data set with comprehensive feature information is used to determine the parameters of test samples to generate a small but effective dataset. 25 textured samples based on L16 (4^4) and L9 (3^4) are fabricated, with the parameter set determined using OAM. COFs of the samples are tested using RTEC tribo-tester. Trend analysis is conducted to investigate the influence of force, frequency, depth and ellipse axis ratio on COF. Multi-linear Regression (MLR) and Gaussian Process Regression are employed. MLR exhibits better prediction accuracy and is integrated with PSO to minimize COF. The error between the experimental and the theoretical results obtained by the integration method of MLR and PSO is only 1.04%, demonstrating the feasibility of predicting COF and optimizing surface texture using the integrated method with a limited dataset determined by OAM.

Keywords

Coefficient of friction, surface texture, machine learning, optimization

Date received: 21 May 2024; accepted: 24 July 2024

Introduction

Water-lubricated Ultra-High Molecular Weight Polyethylene (UHMWPE) bearings have gained increasing attention in various applications due to their advantages, including excellent wearability, self-lubrication, and anti-corrosion properties.[1–3] Recently, a few studies have tried to utilize micro-textures to improve the frictional performance.[4–6] However, research indicates that the performance of these bearings is improved only with appropriate design under specific conditions. Consequently, the optimal design of surface textures fabricated on UHMWPE surfaces for specific operating conditions is crucial for improvement of frictional performance.

A few publications have focused on experimental studies of friction and wear of smooth and textured UHMWPE water-lubricated bearings using pin-on-disk test or reciprocating test.[4,7] However, there are two problems when the researcher depends only on experiments: when there are not enough test samples, it is difficult to using traditional methods to comprehensively and accurately analyze the relationship between the frictional performances and structural as well as operating parameters, and thus could not obtain the frictional performance instantly when parameters change; and in contrast, since fabricating surface textures is time-consuming and expensive, testing too many samples will also be time-consuming and costly, which consequently leads to a long design cycle and makes it difficult to obtain the optimal parameters.

Although much research has been done to theoretically predict friction, tribology is still widely recognized as a field largely driven by empirical evidence and data.[8]

[1]College of Mechanical and Electrical Engineering, Hohai University, Changzhou, PR China
[2]Department of Precision and Microsystems Engineering, Delft University of Technology, Delft, The Netherlands

Corresponding author:
Huihui Feng, College of Mechanical and Electrical Engineering, Hohai University, Changzhou, Jiangsu 213200, PR China; 13200, PR China.
Email: fenghh@hhu.edu.cn

Since the frictional performance of water-lubricated UHMWPE is influenced by the combination of structural parameters and operating conditions, it is not easy to establish a mathematical expression to predict the friction coefficients with varying structural or operating parameters. When the structural parameters of the texture or operating conditions change, it is necessary to prepare new samples and re-test. Therefore, it is necessary to find a method to predict the coefficient of friction at low cost when parameters change.

The recent development of machine learning to perform data analysis introduces the possibility to use these techniques for the prediction of friction performance. In the past few years, researchers have adopted Artificial Neural Networks (ANN), Support Vector Machines (SVM), Random Forest Algorithm (RF) and other ML algorithms to predict the frictional and wear performance of materials based on a dataset obtained from literature or experiments.[8–21] Wang, Zhao, et al.[13] adopted Gradient Boosting Regression Tree (GBRT) to predict COF. Results show that GBRT model produced the excellent predicting accuracy for COF. Bas and Karabacak[8,16] utilized Artificial Neural Network, Support Vector Machine (SVM), and Regression Trees to predict the COF of journal bearings. Performance evaluation showed that ML models can effectively predict COF. Prajapati and Katiyar, et al.[17–19] also used different machine learning algorithms such as ANN, SVM, Classification and Regression Trees (CART), RF and multi-layer perceptron (MLP) model to predict COF and mixed lubrication parameters based on tests and numerical simulations, respectively. Zhao and Wong[20] established a novel method to combine the physics-informed neural network (PINN) and data-driven strategies to predict tribological performance of hydrodynamic lubrication scenario. Prakash Kumar and Binay Kumar[21] employed ANN and multiple linear regression analysis to predict wear rate and COF based on linear reciprocating wear test. Results showed that the model could predict wear behavior effectively.

Due to the high cost of sample manufacturing and friction testing, how to reduce sample size and efficiently get dataset with comprehensive characteristic information for ML is one of the key issues for predicting the friction performance. To solve this problem, a few scholars began to use orthogonal array method (OAM) to determine the combination of sample parameters.[12,22] OAM is an efficient and economical experimental design method considering multi-factors and multi-levels. It is adopted in this study to construct a dataset that ensures covering comprehensive test results using limited sample size and test repetitions. Through carefully designed matrices, OAM systematically covers all combinations of different levels. Compared to full factorial experiments, it significantly reduces the number of tests, saving time and resources. Kim and Yoon[12] designed frictional tests based on OAM (L9). Four-factors and three-levels orthogonal experiment with 9 samples were designed for friction test. The test results were used as a dataset for Gaussian process regression (GPR). The constructed hybrid model could predict fiction performance effectively.

So far, the available research on how surface texture influences the friction performance of UHMWPE water-lubricated bearings is still quite limited. When it comes to textured bearings, the influence of various texturing parameters affect friction under different loads and speeds is very complex. Traditionally, in optimizing designs, multiple combinations of parameters were tested and the one that performs best was selected. This method cannot assure whether the selected combination is the global optimal or not. Moreover, if prediction model of frictional performance is established only using machine learning method, it would require preparing a large number of textured samples and performing friction tests to obtain a sizable dataset. This process is time-consuming and expensive, making it difficult to carry out efficient and reliable optimization designs.

Therefore, it's necessary to optimize texture designs integrated machine learning while using a small but information-rich experimental dataset, skillfully using a limited set of experimental data to attain amplified outcomes with minimized inputs. This approach not only reduces time and costs but also allows for more efficient optimizations.

This research aims to propose a novel integrated process of the OAM, ML algorithm and optimization method for prediction and optimization of COF of water-lubricated copper ball-textured UHMWPE pads. Firstly, 25 cases of test samples are designed using OAM to reduce test numbers and avoid partially, inefficiently test. Based on the small dataset, Multi-linear Regression (MLR) and GPR are adopted to train and predict the COF and compared by Leave-One-Out cross-validation (LOO-CV). The model with higher accuracy is then integrated with particle swam optimization (PSO) method to get the optimal structural and operating parameters. Finally, an experiment is conducted to validate the correctness of the integrated model. The overall flowrate is as follows:

Experimental details

Fabrication of textured UHMWPE samples

Uniform UHMWPE bases with diameter of 25 mm and height of 25 mm were fabricated using precision CNC machine tool. The molecular weight of UHMWPE is 1.5×10^6. Copper balls with diameter of 6 mm which were manufactured by Yueli hardware products company were used as the counterpart. Elliptical and circular textures were fabricated on the UHMWPE surfaces using a femtosecond laser (Femto YL-IR-40 W) operating at a wavelength of 1035 nm and a laser spot size of 32μm. As shown in Figure 2, all patterned areas were 10×10 mm in dimensions. The major axis of the elliptical textures is set at 200μm, the minor axis ranges from 80μm to 200μm with an interval of 40μm. The depth of the dimples is set to 10 μm, 15 μm, 20 μm, 25 μm. And the distance between dimple centers is 0.36 mm.

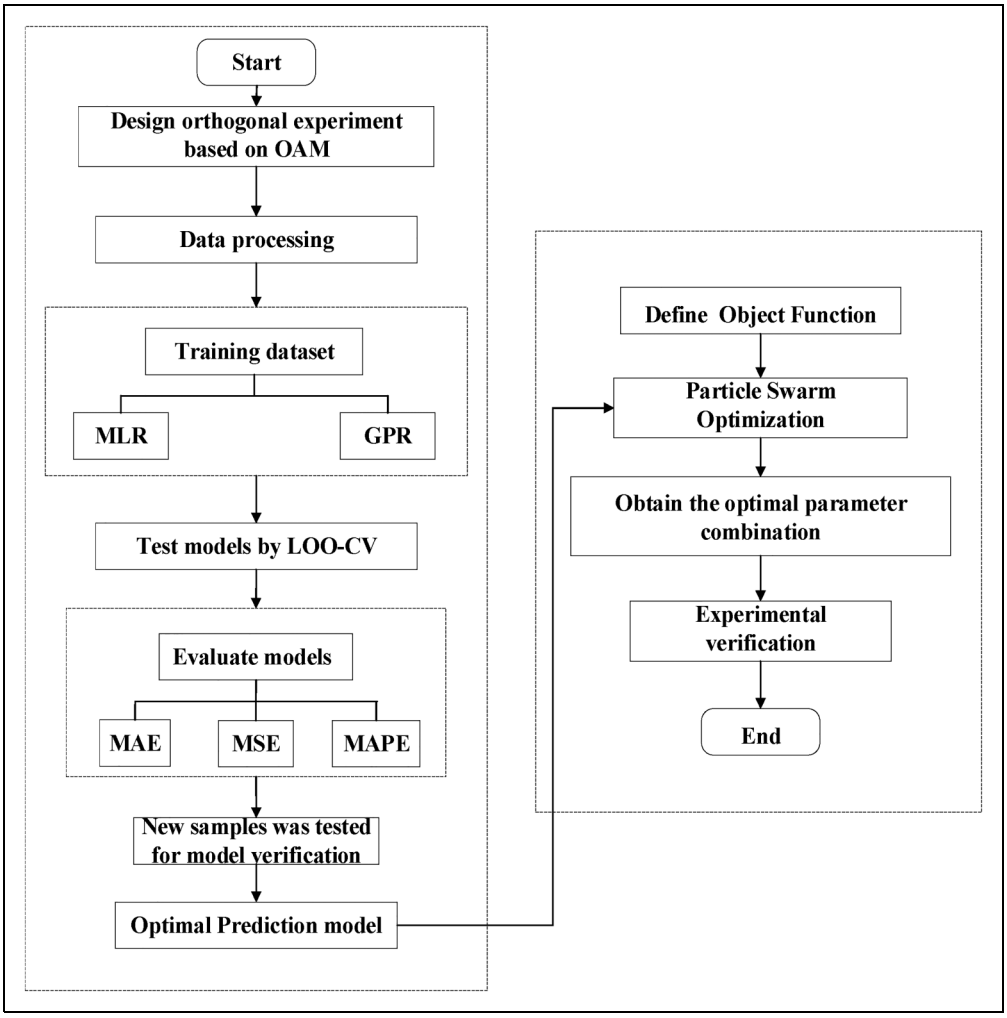

Figure 1. Overall flowrate.

Test facility

All tests were conducted on the RTEC MFT-5000 tribo-tester, which is showed in Figure 3. The UHMWPE samples were installed in a water-containment clamp which was fixed on the platform, and a copper ball is fixed in an axis above the platform. The UHMWPE samples were fully immersed in distilled water. There is a slot at the bottom of the clamp to fix the samples. The platform drives the UHMWPE samples to perform reciprocating motion, which is shown in Figure 3(b). During the tests, the upper copper ball remained stationary once the load applied was settled. The sliding direction is along the major axis of the elliptical textures. The reciprocating stroke of the friction experiment is 4 mm, and the duration for each test is 30 min. The test was repeated 2 times for each condition.

Parameter combinations based on orthogonal array

The applied force, reciprocating frequency which determines the sliding velocity, ratio of minor axis to major axis, and depth of dimple are set as four parameters in the orthogonal array.[22,23] The values for each parameter were determined based on literatures,[4,7,24,25] the manufacturing precision and cost. The ratio of minor axis to major axis (λ) are selected as 0.4, 0.6, 0.8 and 1; the levels of the depth are 10μm, 15μm, 20μm, and 25μm. The levels of the reciprocating frequency are determined by the limits of the test equipment. When it reaches a frequency larger than 15 Hz, water will easily be shaken out from the clamp. So, the sliding frequency ranges from 2.5 Hz to 10 Hz with an interval of 2.5 Hz. As for the force that is applied a range of 0∼10N, based on the results of previous research.

To study the influence of sample size on machine learning results, a four-factor four-level orthogonal test table (L16 (4^4)) and a four-factor three-level orthogonal test table (L9 (3^4)) are designed respectively. The details are listed in Tables 1 and 2.

Friction test results and range analysis

Friction test results

As shown in Figure 4, to show the effect of surface texture on COF of the samples, comparisons between the copper ball-smooth and the copper ball-textured UHMWPE pairs

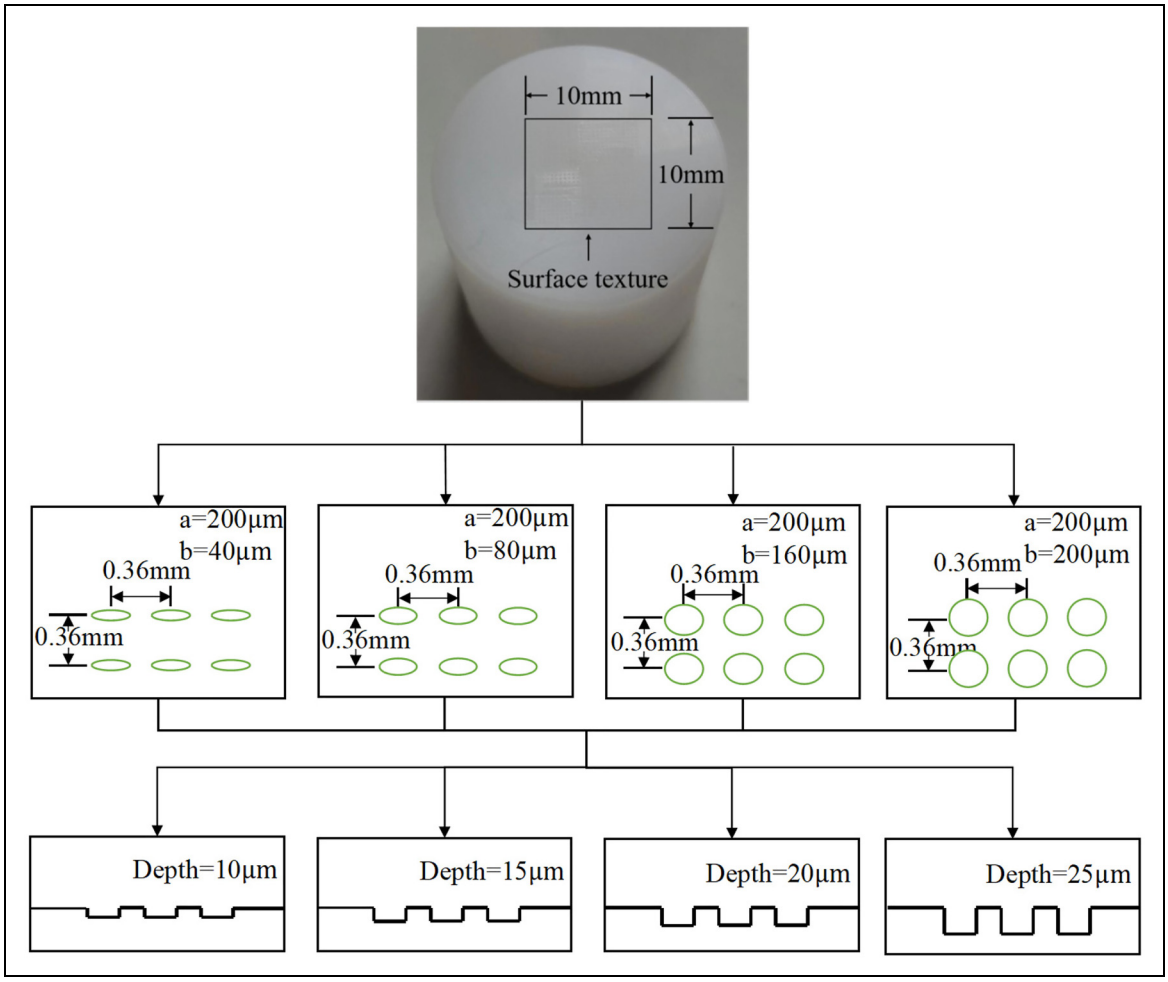

Figure 2. Schematic diagram of the surface textures.

were carried out. The average COFs measured during the period between 20 to 30 min are discussed here to avoid significant fluctuations. Since the test was repeated 2 times for each condition, and the frequency varied, the exact cycles used to calculate the average COFs can be obtained by period*frequency*repeated times. The results of average COFs of each sample can are listed in Tables 3 and 4.

Range analysis of orthogonal results

The range analysis is used to further analyze the orthogonal array results.[26] The average value and influence degree are calculated as follows:

$$\bar{K}_i = \frac{K_i}{n} \tag{1}$$

$$R = \max\left\{ \bar{K}_1 \quad \bar{K}_2 \quad \bar{K}_3 \quad \bar{K}_4 \right\} - \min\left\{ \bar{K}_1 \quad \bar{K}_2 \quad \bar{K}_3 \quad \bar{K}_4 \right\} \tag{2}$$

Where, K is the sum of all the corresponding test friction coefficients when the level number on any column is i, n is the number of levels. R is the influence degree which represents the influence of each factor on COF. The calculated average value $\bar{K}_i$ of the four factors are used as the vertical coordinate and four factors are used as the horizontal coordinate respectively to show the trend of the friction coefficient in respect to the factors. The trend analysis results are shown in Figure 5 and Figure 6.

As shown in Figure 5(a), with the frequency ranging from 2.5 Hz to 10 Hz, the average value $\bar{K}_1$ increase first and then decrease, which is same with that clarified in the reference.[27] When the material of part of the friction pairs is rubber, plastic, et al., the viscoelastic property will exist. The relationship between velocity and friction can be shown as follows[27]:

$$f = (a + bV)e^{(-cV)} + d \tag{3}$$

Where, f is COF and V is the velocity; a, b, c and d are constants corresponding to different sliding materials and different positive pressures. As indicated in the reference,[27] with the increase of the velocity, the COF is combined influenced by the terms $(a + bV)$ and the exponent of a power $e^{(-cV)}$. At first the former part plays a dominant role with increases the friction coefficient and then the latter part plays a dominant role which decreases the

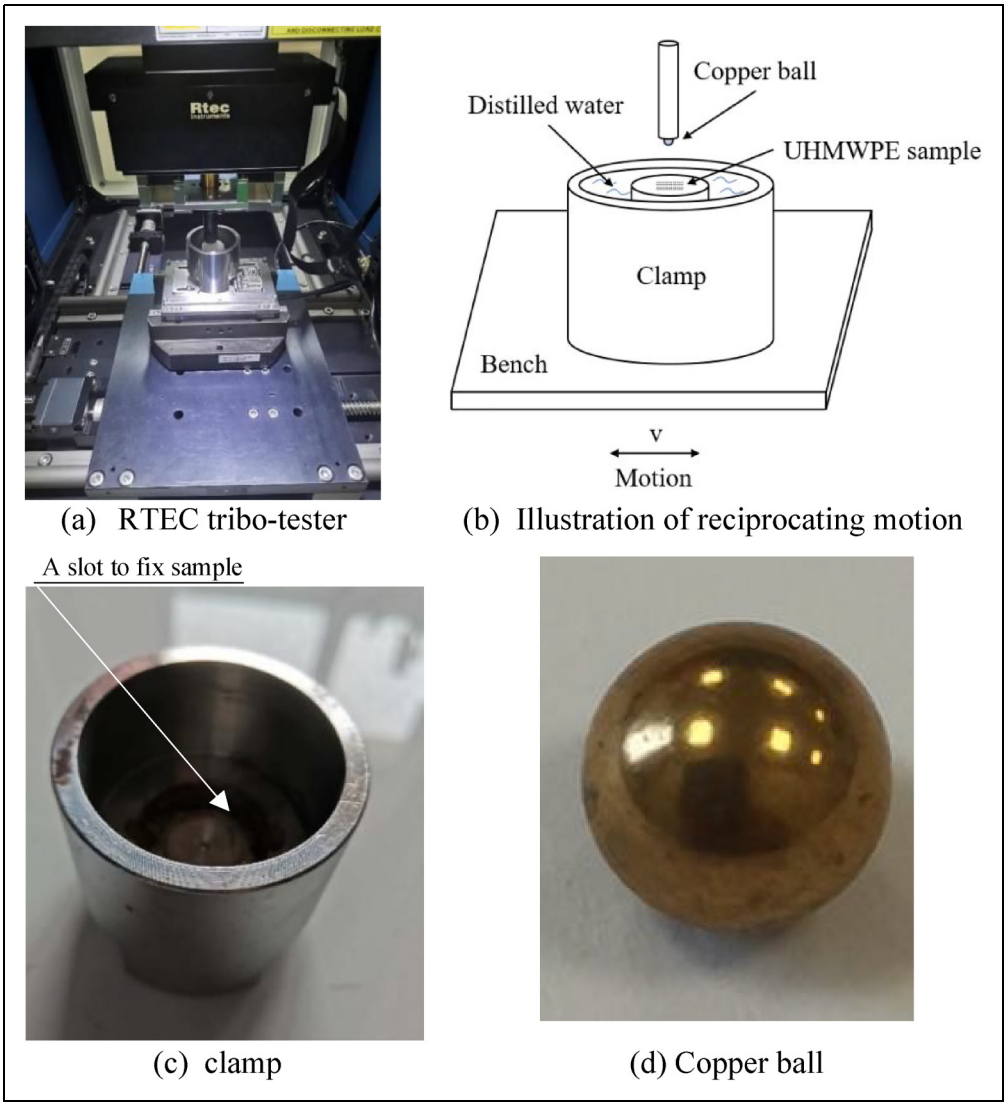

Figure 3. The test facility and illustration of the friction test.

Table 1. The L16 (4^4) orthogonal array design matrix.

Condition	Frequency [Hz]	Force [N]	Depth [μm]	Ratio
1	2.5	1	10	0.4
2	2.5	2.5	15	0.6
3	2.5	5	20	0.8
4	2.5	10	25	1
5	5	1	15	0.8
6	5	2.5	10	1
7	5	5	25	0.4
8	5	10	20	0.6
9	7.5	1	20	1
10	7.5	2.5	25	0.8
11	7.5	5	10	0.6
12	7.5	10	15	0.4
13	10	1	25	0.6
14	10	2.5	20	0.4
15	10	5	15	1
16	10	10	10	0.8

friction coefficient. As a result, the COF increases and then decreases with the velocity.

Table 2. The L9 (3^4) orthogonal array design matrix.

Condition	Frequency [Hz]	Force [N]	Depth [μm]	Ratio
17	7.5	5	10	0.4
18	10	10	15	0.4
19	5	1	20	0.4
20	10	1	10	0.6
21	5	5	15	0.6
22	7.5	10	20	0.6
23	5	10	10	0.8
24	7.5	1	15	0.8
25	10	5	20	0.8

As shown in figures, the COF decreases substantially when the external force increases from 1N to 5N; however, with the external force is further increased, the COF decreases slowly. This is due to that increased load results in a softening of the UHMWPE surface, reduce shear resistance strength of the surface, thus decreasing COF.[28] However, with further increased external load, the UHMWPE surface softens gradually, and

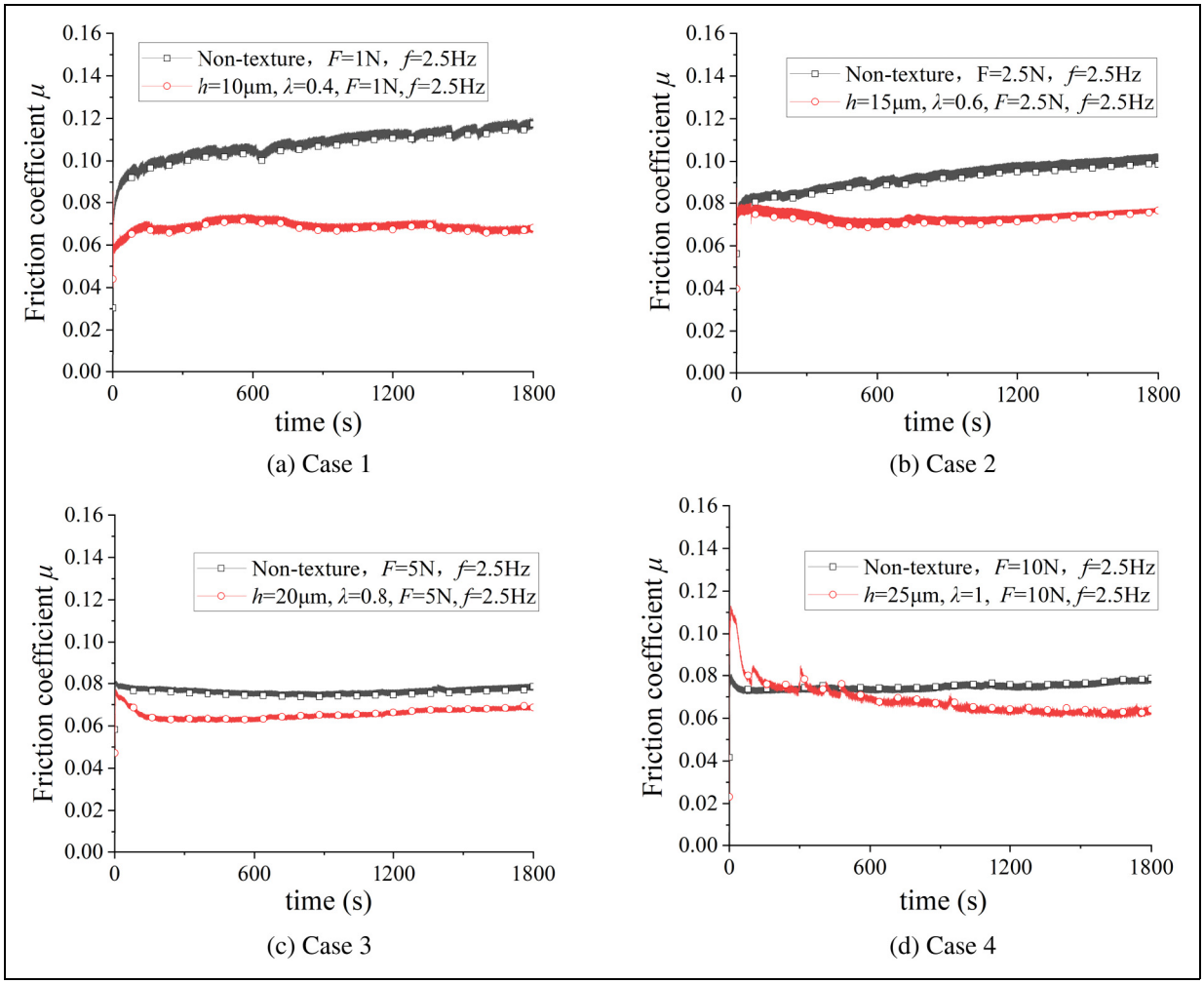

Figure 4. Test results of smooth and textured pairs. (continued)

further pressure therefore can't flatten more asperities. As a result, the contact area is nearly unchangeable at higher pressure.

According to the result, with increasing depth, the COF increases and then decreases. For a shallow dimple, the water film in the dimple will generate extra hydrodynamic force through reciprocating motion; water in the dimples will generate a lift force to the copper ball when it is under squeezed. The shallower the dimple is, the more significant the additional hydrodynamic lift effect is. However, with increased dimple depth, as illustrated in Figure 7, water generates backflow in the deep dimple, reducing the flow into the convergent gap. This weakens the hydrodynamic lubrication effect, resulting in an increase in the COF. However, when the depth of the texture increases to 25um, the COF decreases. The reason for this is that the bottom vortex in the dimple has little effect on the flow when the dimple is deep enough. Under the combined effect of hydrodynamic force and vortex, the friction decreases again.

Figure 5(d) illustrates how COF varies with the ratio λ. According to the result, elliptical dimples outperform circular dimples in reducing friction. When the ratio λ is 1, indicating a circular dimple, the COF is about 0.89; while the COF of the elliptical dimples with ratios smaller than 1 are below 0.80, demonstrating their superior friction-reduction capabilities. For the elliptical dimples, the COF increases first and then decrease.

Friction coefficient prediction based on machine learning methods

MLR and GPR are employed in this study for training the dataset.

Multi-Linear regression

MLR is a statistical method used to deal with more than one independent variable. The relationship between the independent input variables and dependent variable is assumed to be linear and a MLR equation is defined by the following expression[29]:

$$Y = \beta_0 + \beta_1 X_1 + \beta_2 X_2 + \ldots + \beta_n X_n + \varepsilon \quad (4)$$

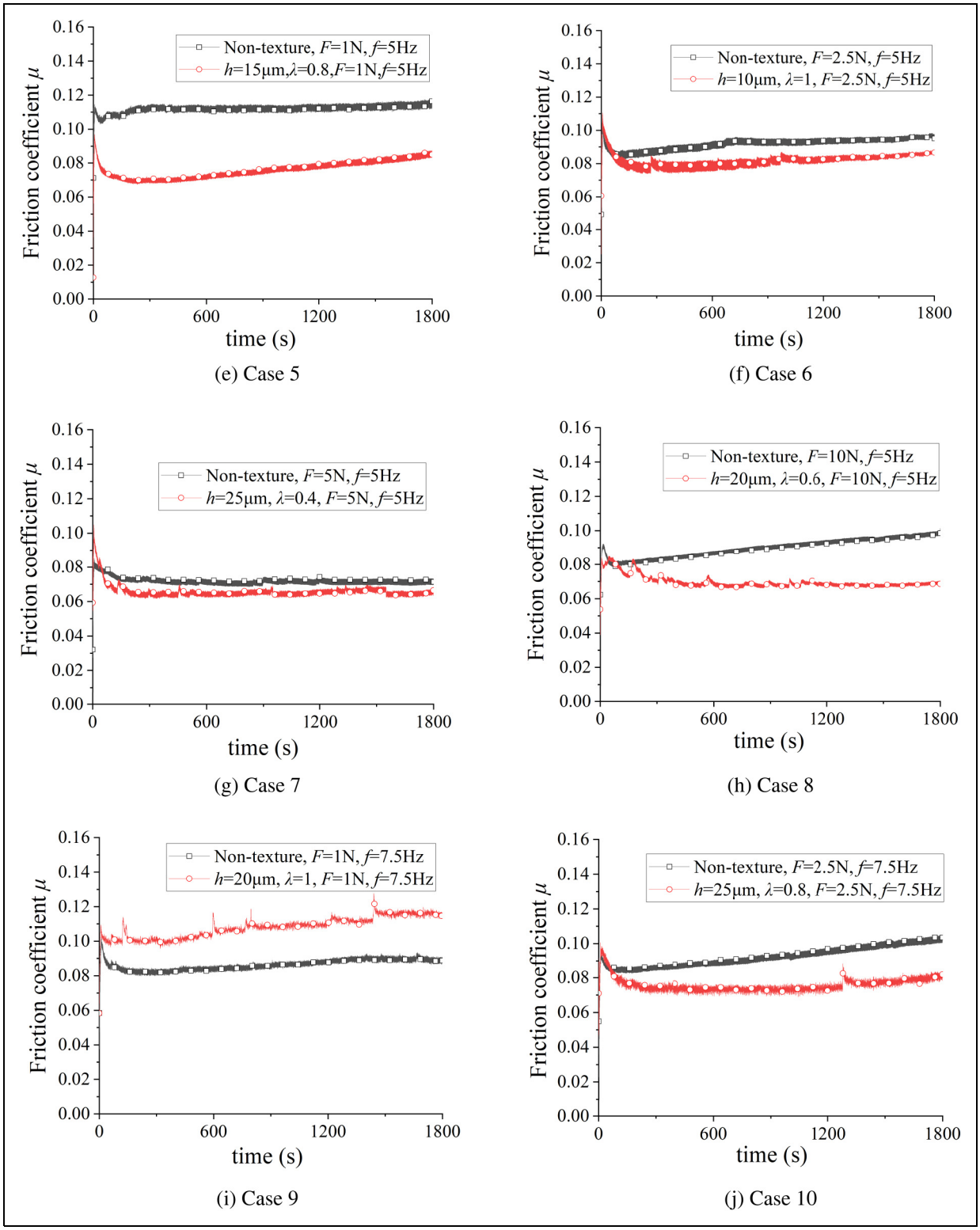

Figure 4. Continued.

where, Y is the dependent variable which will be predicted based on the formula, X_n denotes the independent input variables, β_n is the coefficient reflecting the influence of each independent variable on the dependent variable which can be estimated through least square method, and ϵ is the regression stochastic error.

From the range analysis, it can be seen that the relationship between the COF and each variable is not restrict linear relationship. Therefore, in order to deal with the partially nonlinear relationships, variable transformation is introduced to transform the nonlinear relationship into linear relationship. As analyzed and

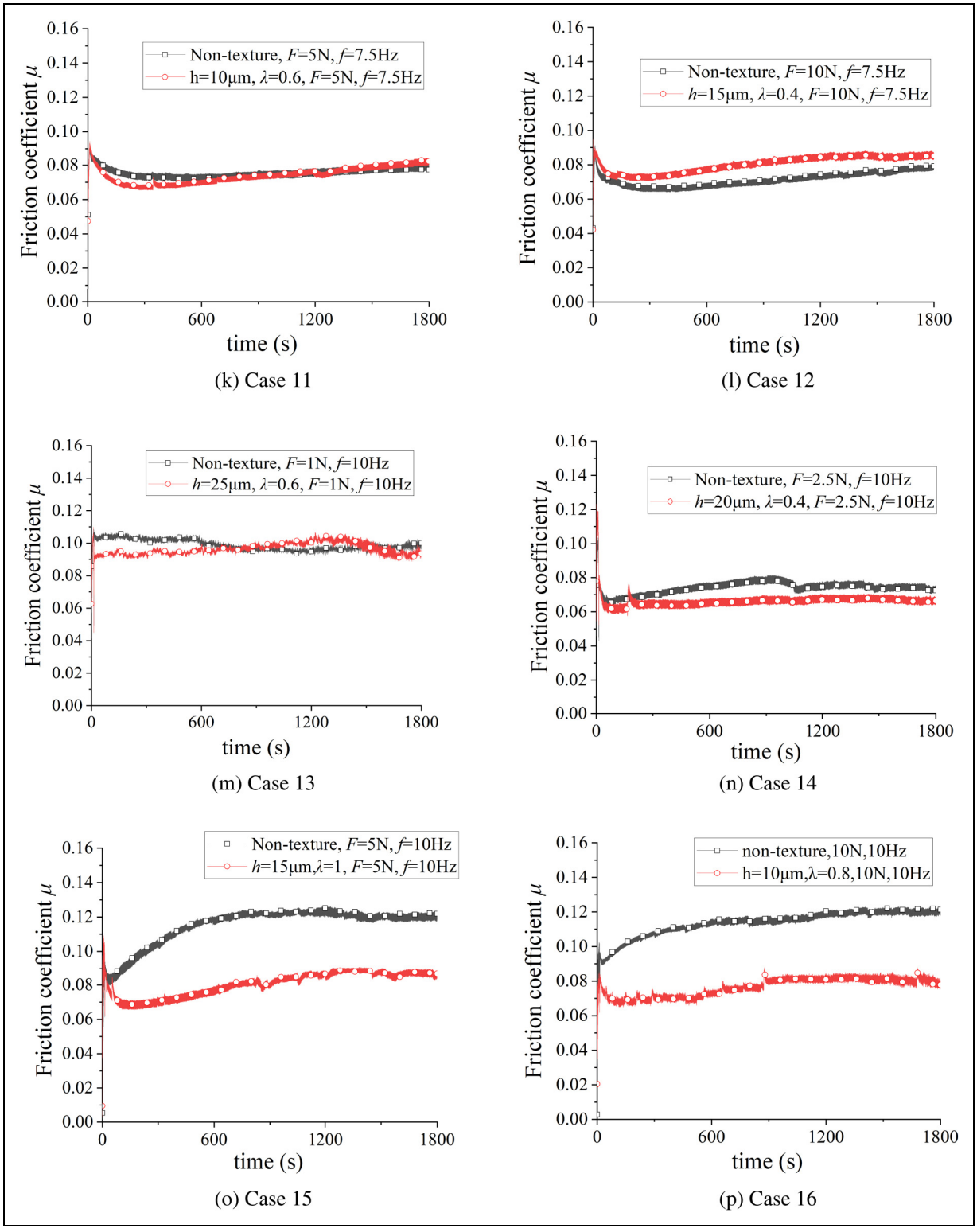

Figure 4. Continued.

discussed in the above section, the COF is the non-linear function of frequency in the form of (e^V, Ve^V) as listed in equations (3). According to the range analysis results, the COF is a linear or partially linear, quadratic or power function of force, depth and ratio of minor to major axis. The expression of COF in terms of single variable can be fitted according to the above results at first.

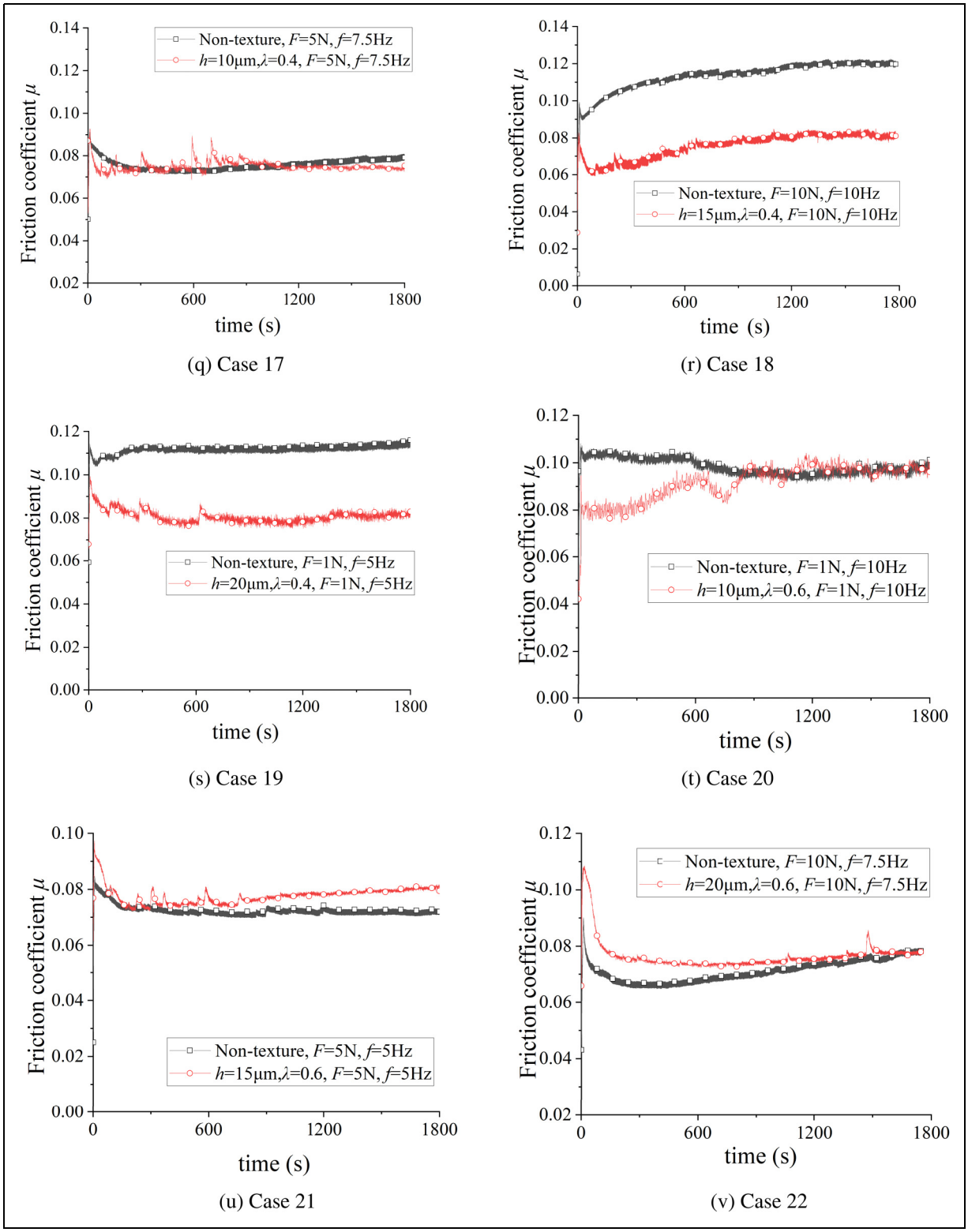

Figure 4. Continued.

As a result, the expression of COF can be fitted in the form of exponential function, quadratic polynomial, power function and other functions:

$$Y = \beta_0 + \beta_1 f(e^{g(v)}, ve^{g(v)}) + \beta_2 f(e^{g(F)}, F^n) + \beta_3 f(h, h^2) + \beta_4 f(e^{g(\lambda)}) + \varepsilon \quad (5)$$

Where, v F, h and λ represent the velocity (frequency), force, depth and ratio of minor to major axis. The fitted functions are packaged as a preprocessor, which are used to transform the nonlinear relationship into linear relationship. The whole of the encapsulated function in respect to a single factor is used as a new variable through preprocessor to establish the MLR model. The

Table 3. Results of L16 (4^4) test.

Cases	speed	force	depth	Ratio of minor to major axis	Cycles	Friction coefficient
1	2.5	1	10	0.4	300	0.068
2	2.5	2.5	15	0.6	300	0.0744
3	2.5	5	20	0.8	300	0.0674
4	2.5	10	25	1	300	0.0669
5	5	1	15	0.8	600	0.0812
6	5	2.5	10	1	600	0.084
7	5	5	25	0.4	600	0.0706
8	5	10	20	0.6	600	0.0692
9	7.5	1	20	1	900	0.1198
10	7.5	2.5	25	0.8	900	0.0838
11	7.5	5	10	0.6	900	0.0785
12	7.5	10	15	0.4	900	0.0849
13	10	1	25	0.6	1200	0.0978
14	10	2.5	20	0.4	1200	0.0840
15	10	5	15	1	1200	0.0872
16	10	10	10	0.8	1200	0.081

Table 4. Results of L9 (3^4) test.

Cases	speed	force	depth	Ratio of minor to major axis	Cycles	Friction coefficient
17	7.5	5	10	0.4	900	0.0744
18	10	10	15	0.4	1200	0.0817
19	5	1	20	0.4	600	0.0808
20	10	1	10	0.6	1200	0.0975
21	5	5	15	0.6	600	0.0794
22	7.5	10	20	0.6	900	0.0773
23	5	10	10	0.8	600	0.0723
24	7.5	1	15	0.8	900	0.0894
25	10	5	20	0.8	1200	0.0904

encapsulated preprocessor is integrated with the MLR model to form a complete predictive model.

Gaussian process regression

GPR is a non-parametric model and developed based on Bayesian and statistical learning theory. It is often used for regression problems with small samples due to its high flexibility.

The distribution of training points and test points is assumed to follow Gaussian distribution[30]:

$$\begin{bmatrix} \boldsymbol{y} \\ y_{N+1} \end{bmatrix} \sim N\left(\begin{bmatrix} \mu(X_N) \\ \mu(X_{N+1}) \end{bmatrix}, \begin{bmatrix} Ke(X_N, X_N) + \sigma^2 I & Ke(X_{N+1}, X_N)^T \\ Ke(X_{N+1}, X_N) & Ke(X_{N+1}, X_{N+1}) \end{bmatrix} \right) \quad (6)$$

Where μ is the mean function, which is usually assumed to be zero, Ke is the covariance function or kernel function. The most used kernel function radial basis function is adopted:

$$k(x, x') = \sigma_f^2 \exp\left[\frac{-(x - x')^2}{2l^2}\right] \quad (7)$$

Where σ_f and l denote hyper-parameters.

Leave-One-Out cross-validation

LOO-CV[31] is usually used in ML to prevent bias due to a particular validation dataset and to reduce the risk of overfitting when there is insufficient data to adopt more efficient techniques like the 3-way split (train, validation and test), especially when the number of the examples in the dataset is less than 50.

The schematic diagram is shown in Figure 8. The COF database is split into a training set and a test set. Then one data is adopted for testing and the remains are used to train the model in each iteration. The procedure is repeated until each data is used once for testing. For each iteration, an evaluation criteria value can be obtained; after all the evaluations, the average evaluation criteria value can be used to evaluate the prediction model.

Performance evaluation for prediction accuracy

In this study, Mean Absolute Error (MAE), Root Mean Squared Error (RMSE) and Mean Absolute Percentage Error (MAPE) are used to compute the error between the real and predicted data[30]:

$$MAE = \frac{1}{n}\sum_{i=1}^{n} |\hat{y_i} - y_i| \quad (10)$$

$$RMSE = \sqrt{\frac{1}{n}\sum_{i}^{n} (\hat{y_i} - y_i)^2} \quad (11)$$

$$MAPE = \frac{1}{n}\sum_{i=1}^{n} \left|\frac{\hat{y_i} - y_i}{y_i}\right| \quad (12)$$

When the value equals to zero, the algorithm has the highest accuracy. Negative or positive values indicate underestimated or overestimated models, respectively.

In order to compare the influence of different sample sizes on machine learning results, predictions based on two datasets are compared. Experimental results No. 1–16 are taken as dataset 1, and experimental results No. 1–25 are taken as dataset 2. Table 5 shows the evaluation performance of the models trained with two different

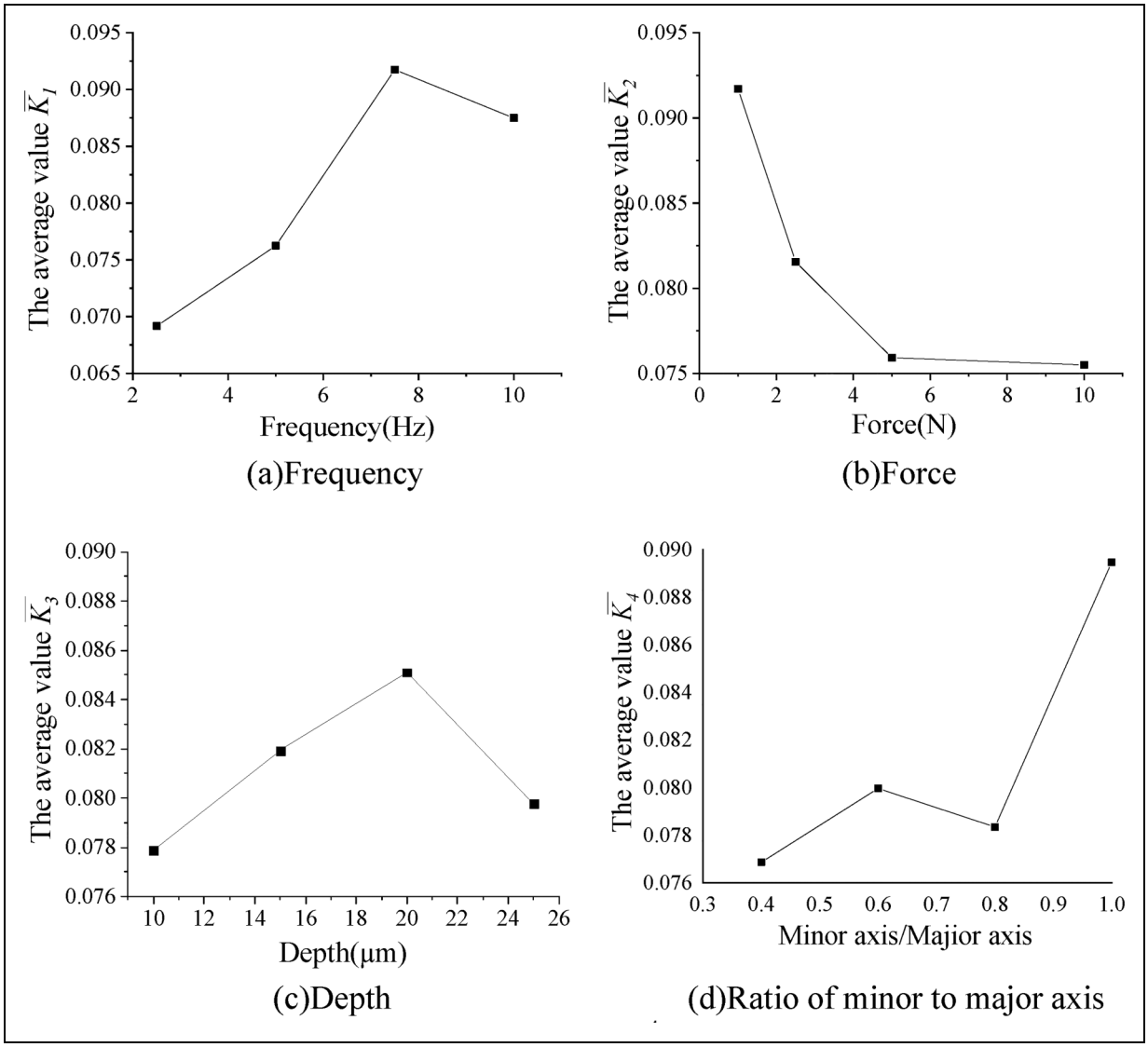

Figure 5. Trend chart of L16 (4^4) experiment.

datasets. According to the result, the prediction model based on dataset 2 is slightly better than that based on dataset 1. The slightly more accurate of predictions based on dataset 2 can be ascribed to the increasing data set. But the overall prediction performance differs a little, which indicates the reliability of the prediction model based on small samples. According to the result, MLR prediction model has a better prediction performance for both of the two data sets. As a result, MLR model will be used for the following optimization.

Test validation of the prediction model

The MLR model trained by the dataset with 25 samples is adopted for the next step. In order to test the generalization performance of MLR and GPR, extra four samples were fabricated and tested. The parameter combinations were shown in Table 6. The result of COF is shown in Figure 9.

The corresponding predicted values and the errors between the predicted and experimental results were listed in Tables 7 and 8. The generalization performance obtained from MLR and GPR algorithms are compared through the difference between the predicted results and the actual experimental values of coefficient of friction. For results of validation test 2, the prediction error obtained by GPR is much smaller than that by MLR, but for the rest of the validation test, the prediction from MLR was more accurate. It could be seen from Figure 9, for test 2, at the last 10minutes, COF hasn't reached a total steady state, while for other tests, COF has already kept to be a relatively steady state. This could be one of the reasons for the inaccuracy in the MLR algorithm for test 2. Furthermore, for MLR, the maximum difference between the prediction and the test results is 4.29%, and the average difference is about 2.56%; while for GPR, the maximum difference reaches as high as 11.29%, and the average difference is about 4.36%, showing the generalization performance of MLR algorithm is much better than that of GPR. Considering the manufacturing error and test error, the prediction results match well with the test results. As a result, the

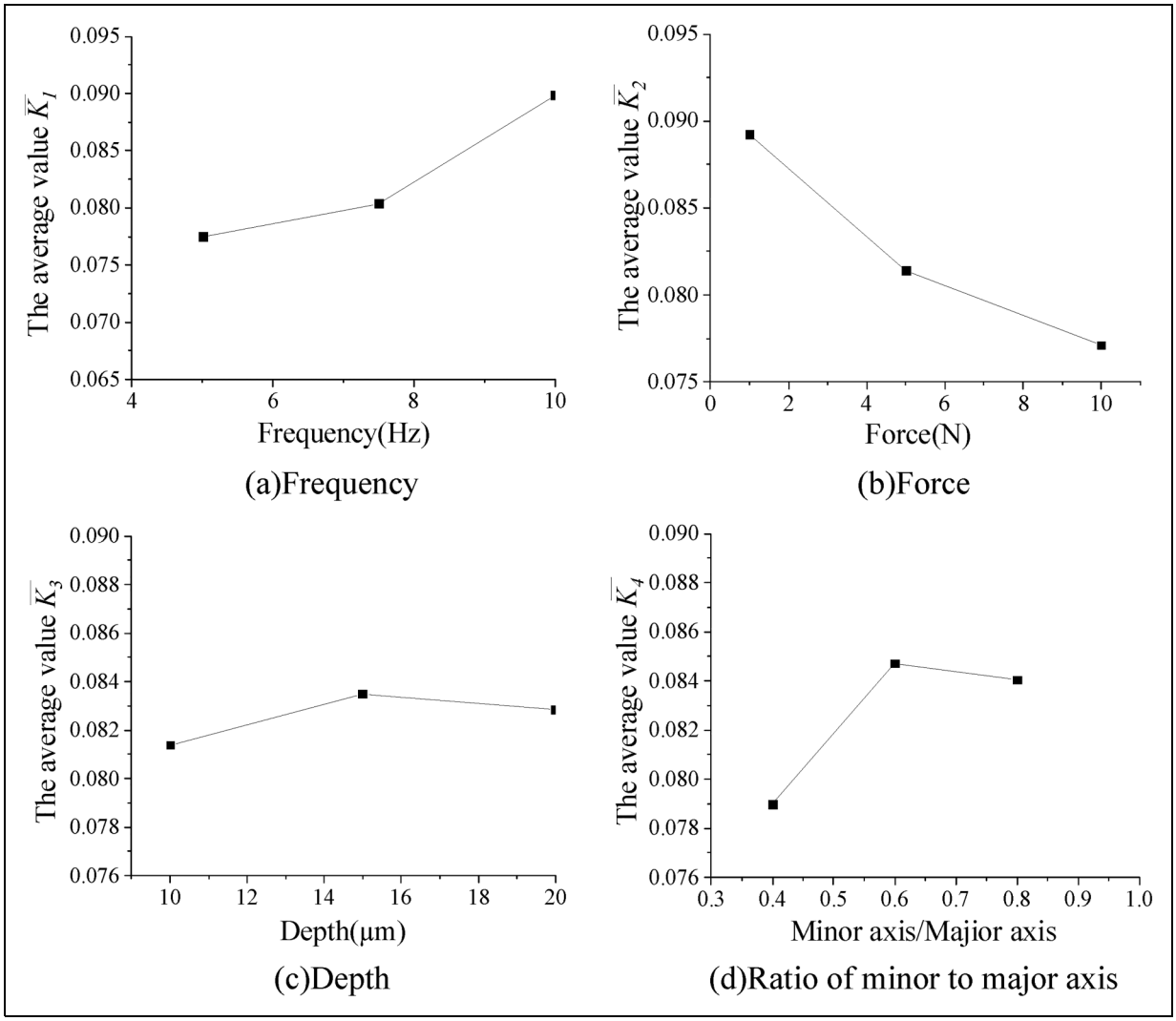

Figure 6. Trend chart of L9 (3^4) experiment.

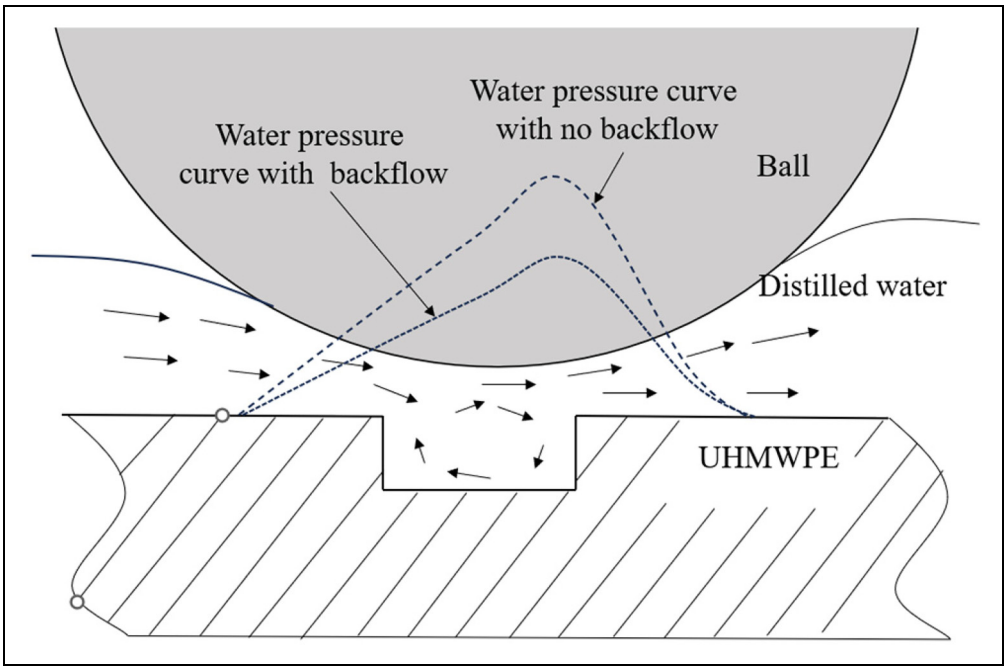

Figure 7. Flow in the dimple and film.

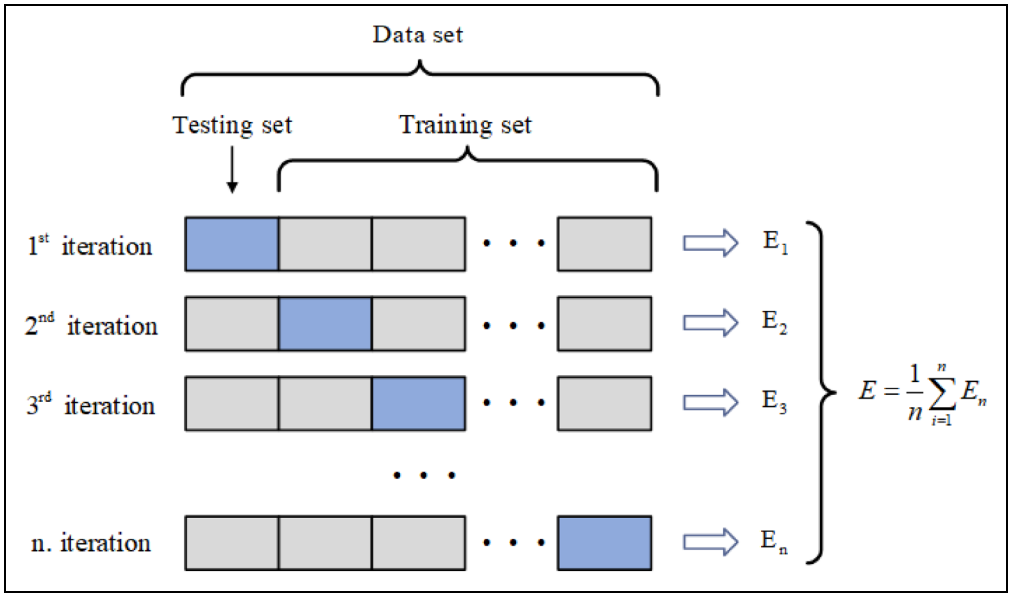

Figure 8. Schematic diagram of LOO-CV.

Table 5. Evaluation indicators.

Model	MAE	RMSE	MAPE
MLR dataset 1	0.007728984	0.011273154	0.088136138
GPR dataset 1	0.010236449	0.013455036	0.116402142
MLR dataset 2	0.005661196	0.008333175	0.065477643
GPR dataset 2	0.008894124	0.013109119	0.099464996

Table 6. Parameter combinations of samples.

Number	speed	force	depth	Ratio of minor to major axis
1	4	3	15	0.4
2	6	5	15	0.6
3	8	7	20	0.6
4	10	9	20	0.8

presented MLR prediction model based on the small dataset could be used to predict the friction coefficient.

Integration with particle swarm optimization algorithm

Based on the results obtained in the previous section, the MLR model is now used in combination with PSO to find out the optimal parameters. The implementation of the PSO algorithm follows the steps below[32]: 1) Define the objective function. The minimization of COF is set as the objective function. 2) Determine the constrictions. The range of frequency, force, depth and ratio is 2.5~10 Hz, 1~10N, 10~25μm and 0.4~1, respectively. 3) Specify parameters of PSO algorithm. The number of particles in each generation is 100 and the maximum iteration number is 1000. 4) Initialization. 5) Evaluate COF of each generation. Based on the COF of each particle predicted by the former established MLR prediction model, find out the best position of the particles. 6) Update velocity and position of particles. 7) Update the global best position. The COFs obtained from the new position and velocity are compared with the current particles' best values. 8) Repeat steps 5–7 until the convergence criteria is satisfied. In this study, the iteration is converged when the difference between the updated global minimum COF and the current minimum COF is smaller than 10^{-8}.

The obtained optimal parameter combination is: the frequency of 2.5 Hz, applied force of 10N, depth of texture of 10μm and the ratio λ of 0.4. The optimal result of the minimum COF is 0.0577156.

Test validation

To validate the whole process proposed in this study, a sample is fabricated with the optimized structural parameters and is tested under the force of 10N and frequency of 2.5 Hz. The tested COF in respect to time is shown in Figure 10. After 20 min running, the average COF is about 0.05712. The error between the test result and the optimization result is only 1.04%, showing the accuracy of the proposed friction prediction process.

Concluding remarks and future prospects

This study proposed a novel integration method of orthogonal array method, ML prediction and particle swarm optimization method to efficiently optimize structural parameters of surface texture under the most appropriate operating condition with minimum coefficient of friction. Firstly, combinations of structural and operating parameters determined using OAM were tested on a RTEC tribo-test. Then, MLR and GPR were used and compared to predict the COF. Finally, a combined approach of the

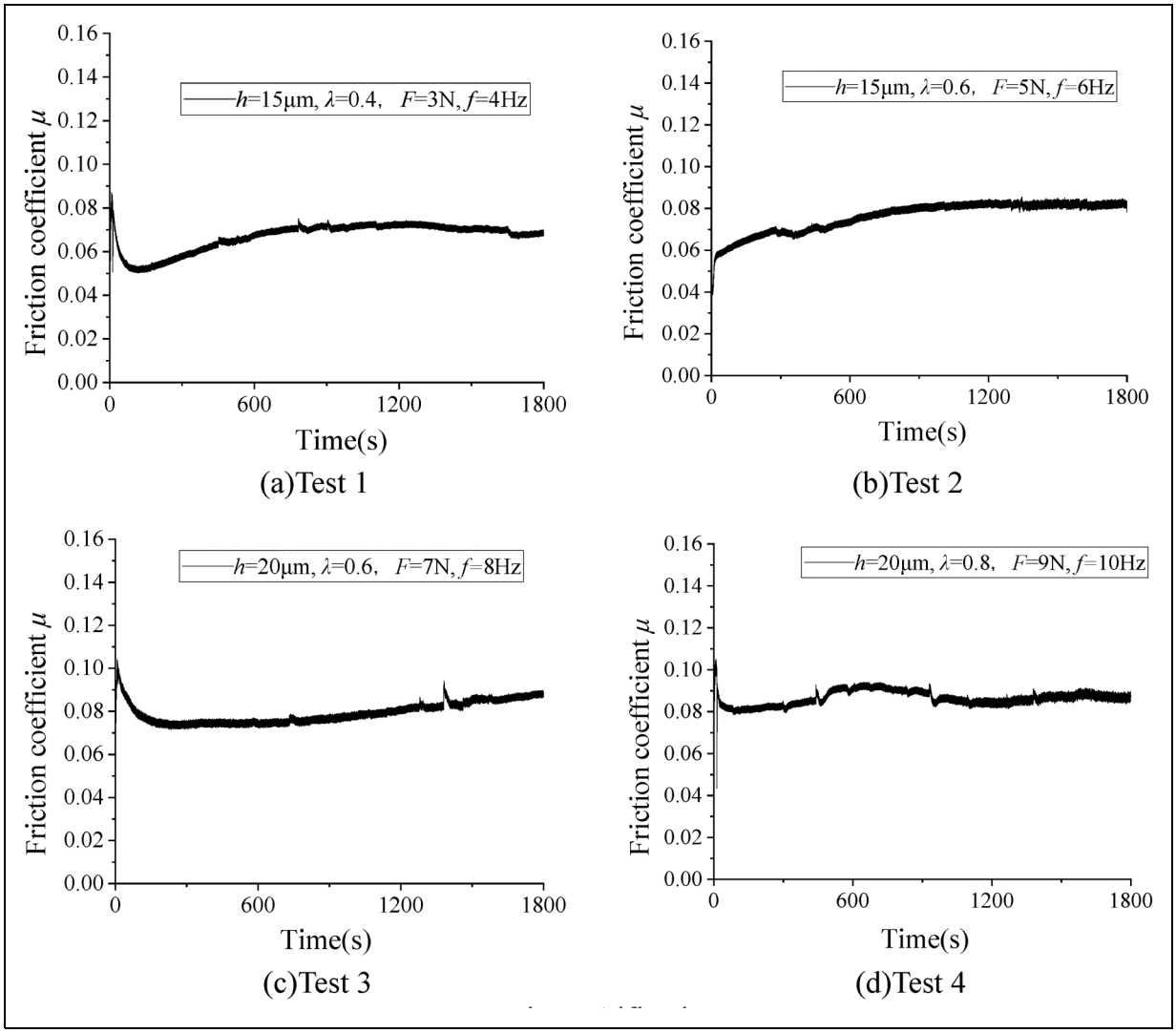

Figure 9. Test verification.

Table 7. Prediction results.

Validation number		1	2	3	4
Experimental value		0.0703	0.0809	0.0843	0.0868
Predicted value	MLR	0.07137301	0.07742742	0.08109981	0.087322
	GPR	0.07823358	0.08037665	0.07966733	0.079068

Table 8. The prediction error.

Validation number		1	2	3	4	Average error (%)
Error (%)	MLR	1.53	4.29	3.80	0.60	2.56
	GPR	11.29	0.64	5.50	8.71	4.36

PSO method and MLR prediction model is proposed to minimize the COF, and the optimization result is validated by comparison with test result. The main conclusions can be summarized as follows.

1. The COF decreases with applied force, while it increases first and then decreases with reciprocating frequency and depth of dimple; elliptical dimples perform better than circular dimples and the COF also increases first and then decreases with an increasing ratio of minor axis to major axis for elliptical dimples.
2. OAM can be effectively used to reduce sample size and efficiently get dataset for machine learning.
3. The MLR method considering the variation of nonlinear relationship shows promising in accurately predicting the COF of copper spheres - UHMWPE pairs based on small dataset obtained by OAM.

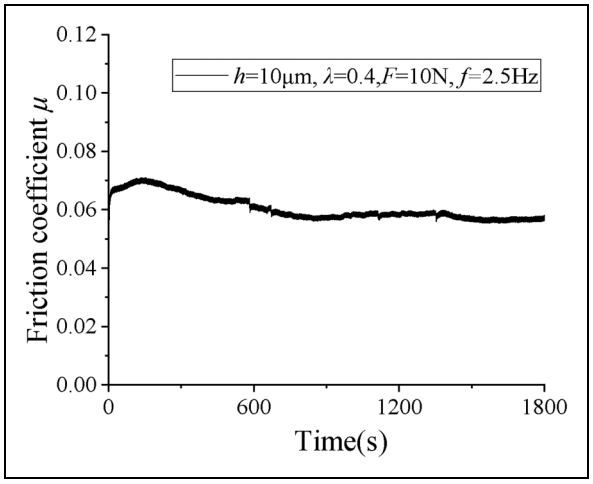

Figure 10. Friction test result of the optimal sample.

4. The error between the experimental and the optimized results obtained by the integration method of MLR and PSO is only 1.04%, showing the effectiveness of the proposed integrated method to minimize the COF.

In future, the process presented here can be extended to predict friction performance of different materials under different conditions and using more advanced algorithms such as Physics-informed Neural Networks. It should be noticed that the integration method offers an alternative approach to design. This method does not mean to replace the exploration of fundamental theoretical mechanisms but serves as a supplementary tool in instances where a comprehensive understanding is yet to be achieved.

Declaration of conflicting interests

The authors declared no potential conflicts of interest with respect to the research, authorship, and/or publication of this article.

Funding

The author disclosed receipt of the following financial support for the research, authorship, and/or publication of this article: This work was supported by the [Fundamental Research Funds for the Central Universities] (grant number B220202025), [Changzhou Sci&Tech Program], grant number (CJ20220099), [National Natural Science Foundation of China] (grant numbers 51705131) and [China Research council] (grant number 202006715009).

ORCID iDs

Huihui Feng https://orcid.org/0000-0002-1903-322X
Ron van Ostayen https://orcid.org/0000-0002-4814-544X

References

1. Chang T, Yuan C and Guo Z. Tribological behavior of aged UHMWPE under water-lubricated condition. *Tribol Int* 2019; 133: 1–11.
2. Wang C, Bai X, Z GUO, et al. Friction and wear behaviours of polyacrylamide hydrogel microsphere/UHMWPE composite under water lubrication. *Wear* 2021; 477: 203841.
3. Xie Z, Jiao J, Yang K, et al. A state-of-art review on the water-lubricated bearing. *Tribol Int* 2023; 18: 108276.
4. Chang T, Guo Z and Yuan C. Study on influence of Koch snowflake surface texture on tribological performance for marine water-lubricated bearings. *Tribol Int* 2019; 129: 29–37.
5. Wu Z, Sheng C, Guo Z, et al. Surface texture processing for tribological performance improvement of UHMWPE-based water-lubricated bearings. *Ind Lubr Tribol* 2018; 70: 1341–1349.
6. Zhang Z, Ouyang W, Liang X, et al. Review of the evolution and prevention of friction, wear, and noise for water-lubricated bearings used in ships. *Friction* 2024; 12: 1–38.
7. Guo Z, Xie X, Yuan C, et al. Study on influence of micro convex textures on tribological performances of UHMWPE material under the water-lubricated conditions. *Wear* 2019; 426: 1327–1335.
8. Baş H and Karabacak YE. Machine learning-based prediction of friction torque and friction coefficient in statically loaded radial journal bearings. *Tribol Int* 2023; 186: 108592.
9. Wu D, Jennings C, Terpenny J, et al. A comparative study on machine learning algorithms for smart manufacturing: tool wear prediction using random forests. *J Manuf Sci Eng* 2017; 139: 071018.
10. Guo F, Cheng G, Yang Z, et al. Deep learning algorithm to predict friction coefficient of matching pairs at different temperature domains based on friction sound. *Tribol Int* 2023; 188: 108903.
11. Hasan MS, Kordijazi A, Rohatgi PK, et al. Triboinformatics approach for friction and wear prediction of al-graphite composites using machine learning methods. *ASME J Tribol* 2022; 144: 011701.
12. Kim Y and Yoon H-S. A model for predicting the friction of micro patterns fabricated by precision machining. *Tribol Int* 2022; 175: 107862.
13. Wang G, Ruan Y, Wang H, et al. Tribological performance study and prediction of copper coated by MoS2 based on GBRT method. *Tribol Int* 2023; 179: 108149.
14. Wang G. Tribological performance prediction of WS2 coating under different conditions by machine learning. *Wear* 2023; 532–533: 205092.
15. Han S, Orzechowski G, Kim J-G, et al. Data-driven friction force prediction model for hydraulic actuators using deep neural networks. *Mech Mach Theory* 2024; 192: 105545.
16. Baş H and Karabacak YE. Prediction of friction coefficient and torque in self-lubricating polymer radial bearings produced by additive manufacturing: a machine learning approach. *Proc Inst Mech Eng J: J Eng Tribol* 2023; 237: 2014–2038.
17. Prajapati DK, Katiyar JK and Prakash C. Machine learning approach for the prediction of mixed lubrication parameters for different surface topographies of non-conformal rough contacts. *Ind Lubricat Tribol* 2023; 75: 1022–1030.
18. Mohammed AS, Dodla S, Katiyar JK, et al. Prediction of friction coefficient of su-8 and its composite coatings using machine learning techniques. *Proc Inst Mech Eng J: J Eng Tribol* 2023; 237: 943–953.
19. Prajapati DK, Katiyar JK and Prakash C. Determination of friction coefficient for water-lubricated journal bearing considering rough surface EHL contacts. *Int J Interact Des Manuf* 2024; 18: 3145–3153.

20. Zhao Y and Wong PPL. A hybrid data-driven approach for the analysis of hydrodynamic lubrication. *Proc Inst Mech Eng J: J Eng Tribol* 2024; 238: 320–331.
21. Kumar P and Kumar B. Synergistic approach to tribological characterization of hybrid aluminum metal matrix composites with ZrB2 and fly ash: Experimental and predictive insights. *Proc Inst Mech Eng E: J Process Mech Eng* 2024. https://doi.org/10.1177/09544089241255931
22. Huang X, Kang N, Coddet P, et al. Analyses of the sliding wear behavior of NiTi shape memory alloys fabricated by laser powder bed fusion based on orthogonal experiments. *Wear* 2023; 534-535: 205130.
23. Gao T, Wang Y, Xie B, et al. The testing and optimization of a bio-inspired textured piston for the BW-250 mud pump. *Polym Test* 2024; 130: 108296.
24. López-Cervantes A, Domínguez-López I, Barceinas-Sánchez JDO, et al. Effects of surface texturing on the performance of biocompatible UHMWPE as a bearing material during in vitro lubricated sliding/rolling motion. *J Mech Behav Biomed* 2013; 20: 45–53.
25. Xu Y, Zheng Q, Abuflaha R, et al. Influence of dimple shape on tribofilm formation and tribological properties of textured surfaces under full and starved lubrication. *Tribol Int* 2019; 136: 267–275.
26. Wang Z, Zhao C and Zhang W. Multi-objective design and optimization of squeezed branch pile based on orthogonal test. *Sci Rep* 2023; 13: 22508.
27. Moore DF. *Principles and applications of tribology*. Oxford: Pergamon, 1975, https://doi.org/10.1016/C2013-0-02605-9.
28. Abdelbary A and Li C. *Principles of engineering tribology*. Cambridge, MA: Academic Press, 2023, https://doi.org/10.1016/C2021-0-01365-1.
29. Hosseini SH, Movahednejad MH and Rohani A. Predicting the scouring depth around a rectangular pier with a round nose by artificial intelligence methods. *Eng Appl Artif Intel* 2024; 133: 108649.
30. Elsheikh AH. Applications of machine learning in friction stir welding: prediction of joint properties, real-time control and tool failure diagnosis. *Eng Appl Artif Intel* 2023; 121: 105961.
31. Pang Y, Wang Y, Lai X, et al. Enhanced Kriging leave-one-out cross-validation in improving model estimation and optimization. *Comput Methods Appl Mech Eng* 2023; 414: 116194.
32. Besharatian B, Tajmir Riahi H, Garcia R, et al. Particle swarm optimization of friction tuned mass dampers subjected to ground motion records. *Soil Dyn Earthq Eng* 2023; 172: 107995.

Nomenclature

b	Scalar
c_1, c_2	Learning factors
f	Reciprocating frequency
r_1, r_2	Random vectors between 0∼1
$v_i^{(k+1)}$	The velocity to be applied to the ith particle in the next step
ω	Inertia weight
$\mathrm{w_s}$	J dimension vector
x	Values for each parameter
$x_{\max}$	Maximum value
$x_{\min}$	Minimum value
$x_i^{(k+1)}$	The position to be applied to the ith particle in the next step
$\hat{y}_i$	The prediction result
y_i	Real data
C	Penalty of error
$\bar{K}_i$	Calculated average value
Ke	Covariance function or kernel function
N	Number of the training data
R	Influence degree of each factor on the friction coefficient
X_n	Independent input variables
Y	Dependent variable
ϵ	Regression stochastic error
β_n	Coefficient reflecting the influence of each independent variable on the dependent variable
μ	Mean function
ξ_i	Distance between the margin and the data points
σ_f, l	Hyper-parameters